J. Electrochem. Sci. Eng. **16** (2026) 3150; https://doi.org/10.5599/jese.3150

Open Access : : ISSN 1847-9286
https://pub.iapchem.org/ojs/index.php/JESE

Original scientific paper

Electrochemical sensing of atenolol using silver-reduced graphene oxide carbon paste nanocomposite electrode

Nevila Broli✉, Sadik Cenolli, Loreta Vallja, Majlinda Vasjari, Ana Ameda and Lueda Kulla

Department of Chemistry, Faculty of Natural Sciences, University of Tirana, Tirana, Albania and NanoAlb, Center of Nanomaterials and Nanotechnology, Academy of Science of Albania, Tirana, Albania

Corresponding Author: ✉nevila.broli@fshn.edu.al

Received: December 4, 2025; Accepted: January 12, 2026; Published: January 20, 2026

Abstract

Atenolol, one of the most prescribed β_1-selective adrenergic blockers, has been increasingly detected in aquatic ecosystems due to incomplete elimination in sewage treatment plants, posing an ecotoxicological hazard to the environment. Here, an electrochemical sensor based on silver-decorated reduced graphene oxide composite carbon paste electrode (rGO@Ag-CPE) was designed for the ultrasensitive electroanalytical determination of atenolol in real-world samples. The morphology and chemical composition of rGO@Ag-CPE were investigated by transmission electron microscopy and energy-dispersive spectroscopy analyses, while the electrochemical properties were evaluated by cyclic and square wave voltammetry techniques. The rGO@Ag-CPE demonstrated excellent electrocatalytic performance toward Atenolol oxidation, attributed to the unique properties of reduced graphene oxide and silver nanoparticles, which provide high conductivity and efficient electrocatalysis, thereby helping to prevent unwanted Atenolol degradation. Under optimized electrochemical sensing conditions, the rGO@Ag-CPE sensor exhibited a linear dynamic range of 20-859 µM (R^2 = 0.9953), a low detection limit of 2.9 µM, and good reproducibility (relative standard deviation < 4.0 %). A validation study on real-world samples showed good atenolol recovery of 88.8-102% in natural waters and 97-99.2 % in pharmaceutical tablets.

Keywords

β-blocker; electrochemical sensor; modified carbon paste electrode; hybrid nanocomposite; voltammetry techniques; real samples

Introduction

Atenolol (ATN) is a selective β_1-adrenergic receptor blocker broadly prescribed for the treatment of hypertension, angina pectoris, and the prevention of myocardial infarction [1]. In the past decade, its frequent detection in aquatic systems has become an environmental concern, as β-blockers disrupt

normal physiological functions and endocrine balance in aquatic organisms [2,3]. Several studies have consistently reported its persistence in both surface and ground water, largely due to incomplete removal by conventional wastewater treatment processes [4-7]. This environmental persistence underlines the need for sensitive and selective analytical methods that are also practical for routine and field-based monitoring.

Among the already existing analytical approaches, GC-MS and HPLC remain the most reliable for atenolol quantification [8-10]. While they are highly precise and reproducible, their use is often limited by complex sample pretreatment, expensive instrumentation, and poor portability [11]. In this regard, electrochemical sensors have increasingly emerged as cost-effective alternatives, featuring fast response times, simple operation, and broad applicability in both pharmaceutical and environmental analysis [12-17].

Considerable efforts were made to improve the electrochemical response of the modified electrodes for ATN detection. For instance, a carbon paste electrode modified with a nanocomposite of reduced graphene oxide/titanium dioxide (rGO/TiO_2/CPE) exhibited outstanding sensitivity, with a detection limit of 0.05 μM in pharmaceutical samples [18,19]. Electrodes modified with superparamagnetic iron oxide nanoparticles (SPIONs) also show excellent repeatability and analytical precision [20-22]. Other related studies involving various composites, such as carbon nanotubes and metal oxides, have also demonstrated promising detection of β-blockers, including propranolol and other similar compounds [23-27]. Overall, these studies demonstrate that nanostructured materials significantly improve the analytical performance of electrochemical sensors by enhancing their sensitivity, selectivity, and operational stability.

Among carbon-based materials, rGO exhibits higher conductivity, a larger specific surface area, and oxygen-containing groups, which enable rapid electron exchange at the electrode interface [28-33]. The combination of rGO with silver nanoparticles (AgNPs) enhances these characteristics, resulting in hybrid materials with improved catalytic activity and charge-transfer efficiency [31-37]. Thus, for instance, a sensitivity of 35.25 μA μM^{-1} cm^{-2} toward 4-nitrophenol detection was reported for an rGO-halloysite-AgNP composite [31], while graphene-AgNP-based sensors have also demonstrated excellent selectivity toward β-blockers in biological matrices [32,34,37]. More recently, rGO/Ag nanocomposites have demonstrated structural robustness and superior electrochemical performance, thus opening further perspectives on the use of such nanostructured composites for analytical sensing [38-47]. In this work, a silver-decorated reduced graphene oxide-modified carbon paste electrode (rGO@Ag-CPE) was prepared and characterized systematically for the voltammetric determination of atenolol. TEM and EDS were used to analyse the nanocomposite morphology and composition, while the electrochemical characteristics were investigated by cyclic voltammetry and square-wave voltammetry. The proposed rGO@Ag-CPE sensor has demonstrated high sensitivity, a low limit of detection, and reliable reproducibility. The present results indicated that the developed composite electrode offers a cost-effective, stable sensing platform suitable for the quantitative determination of β-blockers in pharmaceutical and environmental matrices.

Experimental

Reagents and materials

All chemicals and reagents used were of analytical grade and obtained from reputable suppliers. Pure atenolol (ATN, Standard Series 00336) was used for the preparation of calibration and working solutions. Sulfuric acid (H_2SO_4, 99 %) was purchased from Merck (KGaA, Darmstadt, Germany) and used to prepare the acidic supporting electrolyte. In addition, an acetate buffer at pH 4.5 (0.1 M acetic acid +

+ 0.1 M sodium acetate) was used for cyclic voltammetry (CV) characterization with the iron redox probe, while an acetate buffer at pH 5.0 was used for optimization of atenolol (ATN) oxidation. Phosphate-buffered saline (PBS) at pH 7.0 (0.1 M phosphate, 0.15 M NaCl) and phosphate buffer (PB) at pH 8.0 (0.1 M phosphate) were used to study the effects of the supporting electrolyte and pH on ATN oxidation. Carbon paste was formulated by mixing synthetic graphite powder (99.9 % purity, particle size 71 to 90 µm; Alfa Aesar, Thermo Fisher Scientific, MA, USA) with paraffin oil (Olio di Vaselina; Zeta Farmaceutici, Sandrigo, Italy). Reduced graphene oxide (rGO) was synthesized from commercial graphene oxide (GO powder, S-methods (≥99.9 % purity), purchased from ACS Material, LLC, Medford, MA; SKU: GNOS0010/ used as received without further purification, *via* a modified Hummers' method, as described in our previous works [40,48,49], and decorated with silver nanoparticles using $AgNO_3$ (≥99.9 %; Sigma-Aldrich) as precursor. A stock solution of atenolol (10 mmol L^{-1}) was freshly prepared in 100 mmol L^{-1} H_2SO_4, stored at 4 °C, and diluted as needed with double-distilled water.

Apparatus and characterization

Electrochemical measurements were performed using a PalmSens 4 electrochemical analyser (PalmSens BV, The Netherlands) in a conventional three-electrode setup, comprising carbon paste electrode (CPE) variants as the working electrode, bare CPE, rGO-modified CPE (rGO-CPE), and silver-decorated rGO-modified CPE (rGO@Ag-CPE); Ag/AgCl (saturated KCl) as the reference electrode, and a platinum wire as the counter electrode. Morphological characterization of the rGO-CPE and rGO@Ag-CPE nanocomposites was conducted by transmission electron microscopy (TEM). For TEM analysis, a small aliquot of a diluted aqueous dispersion of each material was deposited onto copper grids coated with a formvar/carbon support film and air-dried. TEM images were acquired using a JEOL JEM-2100 instrument at an accelerating voltage of 200 kV. The elemental composition and distribution of the rGO@Ag-CPE were further assessed by energy-dispersive X-ray spectroscopy (EDS) coupled with TEM, enabling identification and semi-quantitative analysis of the constituent elements.

Electrochemical measurements

All voltammetric experiments were performed in 15 mL of 100 mmol L^{-1} H_2SO_4 (pH 2) as the supporting electrolyte at room temperature (25 ± 1 °C). Cyclic voltammetry (CV) was used for the electrochemical characterization of the modified electrodes at a scan rate of 100 mV s^{-1}. Square-wave voltammetry (SWV) was employed to evaluate the analytical performance of the electrodes. SWV parameters were optimized as follows: pulse amplitude = 50 mV, frequency = 25 Hz, and potential step = 4 mV in the potential range of 1.0 to 1.8 V *vs.* Ag/AgCl. Before each measurement, the solution was allowed to stabilize for 10 s, and standard additions of atenolol were performed without replacing the supporting electrolyte. Experiments were conducted in triplicate to ensure repeatability, and relative standard deviation (RSD) values were calculated to assess precision.

Preparation of electrodes

Bare carbon paste electrode

The bare CPE was prepared by mixing 1.00 g of graphite powder (70 to 90 µm) with 300 µL of paraffin oil to form a homogeneous paste. The paste was packed into a plastic syringe (8 mm inner diameter) containing a copper wire as an electrical contact.

Reduced graphene oxide - carbon paste electrode

Reduced graphene oxide (rGO) was synthesized using a modified Hummer's method, as described in our previous publications [48,49]. To prepare the rGO-CPE electrode, 100 mg of the synthesized rGO

was added to the graphite powder/paraffin mixture and thoroughly blended to obtain a uniform paste. The paste was then packed into the electrode holder, and the surface was smoothed prior to use.

Reduced graphene oxide/Ag-carbon paste electrode

The rGO@Ag nanocomposite was synthesized by dispersing 0.108 g of rGO and 0.301 g of $AgNO_3$ in 20 mL of distilled water under magnetic stirring for 2 h, followed by ultrasonication for 4 h. During the synthesis process, residual oxygen-containing functional groups on rGO (-OH, -COOH) acted as mild reducing agents, enabling the in-situ reduction of Ag^+ to Ag^0 nanoparticles, as previously reported for graphene-based nanocomposites [42,48-52]. No additional chemical reducing agent was employed. The resulting dispersion was centrifuged at 5000 rpm for 5 min, and the obtained precipitate was dried at 80 °C and stored in a desiccator. For electrode preparation, 100 mg of the pre-synthesized rGO@Ag nanocomposite was mixed with 1.00 g of graphite powder and 300 µL of paraffin oil to obtain a homogeneous paste, which was packed into the electrode body and smoothed prior to use.

Preparation and analysis of real samples

For pharmaceutical analysis, five commercial atenolol tablets (100 mg each) were weighed, finely ground, and homogenized. An amount corresponding to the mean weight of one tablet (0.4196 g) was dissolved in 50 mL of 100 mM H_2SO_4. Aliquots of 0.25 mL of this stock solution were introduced into the electrochemical cell containing 15 mL of 100 mM H_2SO_4 for SWV measurements. Quantification was performed using the standard addition method.

The following procedure was performed for environmental analysis: filtration of Osumi River water samples collected from four sites in Albania, spiking with known concentrations of atenolol (340 and 503 µM), and analysis using the same SWV protocol. Recovery tests and RSD, % were calculated to assess matrix effects and method accuracy.

Results and discussion

Morphological and elemental characterization

Transmission electron microscopy and energy-dispersive X-ray spectroscopy have been used to illustrate the morphology and composition of the synthesized Ag@rGO-CPE nanocomposite. The TEM images of variable scale bars (Figures 1(a)-(d) show transparent, thin, and wrinkled sheets of reduced graphene oxide (rGO) with dark, spherical silver nanoparticles (AgNPs) uniformly dispersed over them. The particles are distinctly visible as dark spots on the rGO surface and are homogeneously anchored to it, confirming the decoration of graphene oxide with AgNPs within the carbon paste matrix. Furthermore, there is no remarkable agglomeration observed, demonstrating that AgNPs have been stably incorporated onto the rGO sheets. Such a uniform and stable distribution indicates strong interactions between rGO and AgNPs, resulting in a well-integrated nanocomposite structure within the carbon paste electrode.

The wrinkled, layered morphology of rGO provides a high surface area and sufficient sites for anchoring nanoparticles, whereas AgNPs embedded within it increase the composite's electrical conductivity and catalytic properties. Such synergistic architecture is highly beneficial for electrochemical sensing, as it enables efficient charge transfer and increases the density of active sites, thereby generally improving sensor performance parameters such as sensitivity and stability. Similar nanostructured composites have been reported for electroanalytical applications involving noble-metal-carbon hybrid materials [39-44].

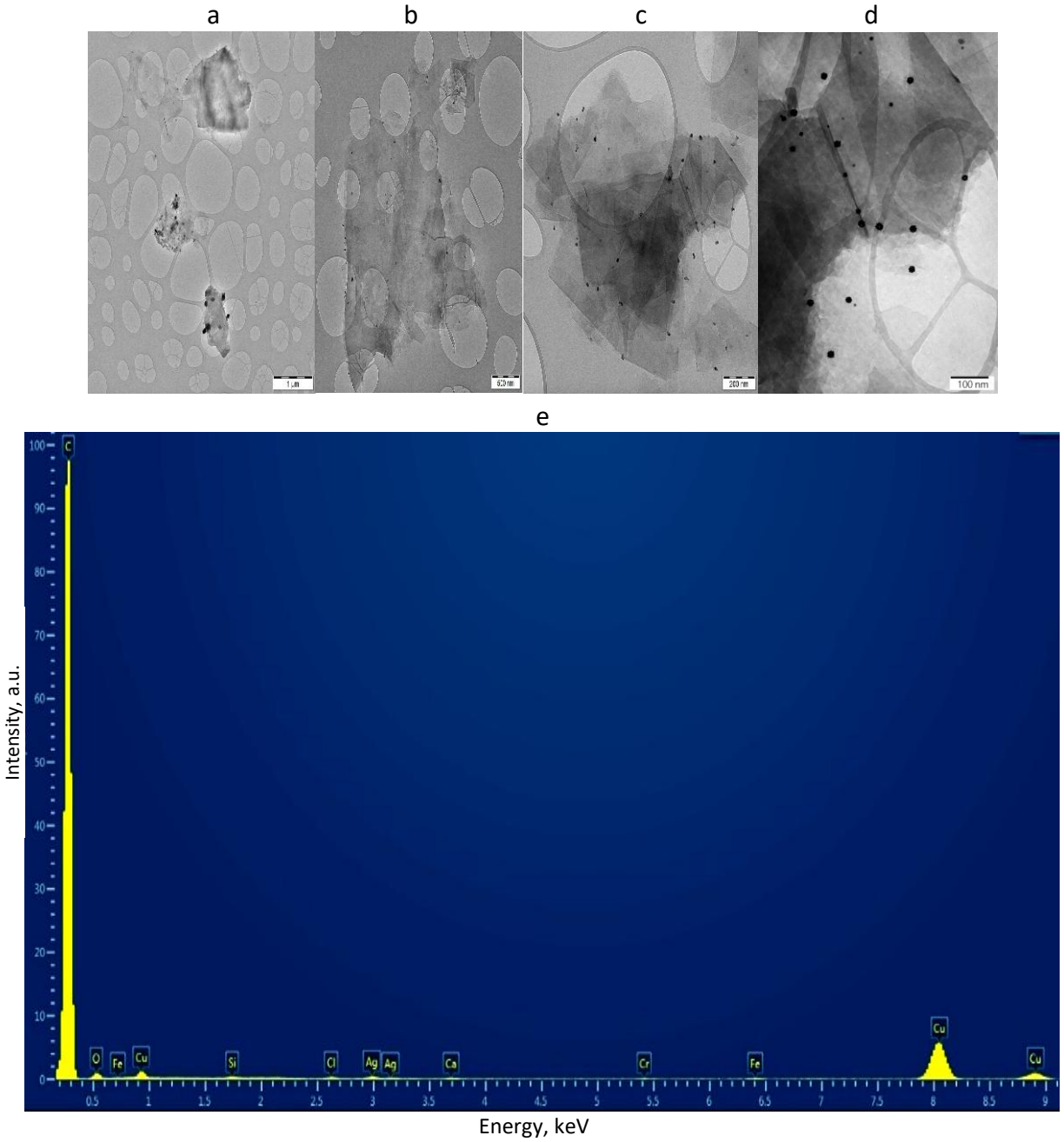

Figure. 1. *Transmission electron microscopy images of rGO@Ag-CPE nanocomposite with different magnifications (a to d), Ag nanoparticles appear as black dots dispersed across rGO sheets; e - EDS spectrum that confirms the presence of C, O and Ag in the composite*

The EDS spectrum in Figure 1e confirms the presence of carbon (C), oxygen (O) and silver (Ag) as the main constituent elements of the rGO@Ag composite. The Ag-related signal observed at around 3 keV verifies the incorporation of metallic silver into the composite structure. Although silver peaks are less intense than carbon peaks, this behaviour is expected given the low loading and high dispersion of Ag nanoparticles, whose contribution is mainly catalytic rather than producing a dominant elemental signal. The absence of additional impurity-related peaks suggests that the synthesized composite is free from detectable contaminants.

Overall, the EDS results clearly demonstrate the successful incorporation of Ag nanoparticles into the rGO matrix, forming a hybrid nanocomposite favourable for electrochemical sensing applications, particularly for the detection of β-blocker molecules such as atenolol.

Electrochemical characterization

To assess the improvement in electrocatalytic capability achieved through electrode modification, cyclic voltammetry was conducted in an acetate buffer solution with pH 4.5 in the presence of 2.7 mM $[Fe(CN)_6]^{4-}$ at a scan rate of 100 mV s^{-1}. As shown in Figure 2, the bare CPE exhibited the lowest redox peak current intensities and the highest peak-to-peak separation, indicating low electron transfer rates at the electrode/electrolyte interface. Following modification with either Ag nanoparticles and rGO, there was an observable increase in current intensity due to enhanced conductivity and electrochemical properties after the addition of Ag nanoparticles and rGO, respectively.

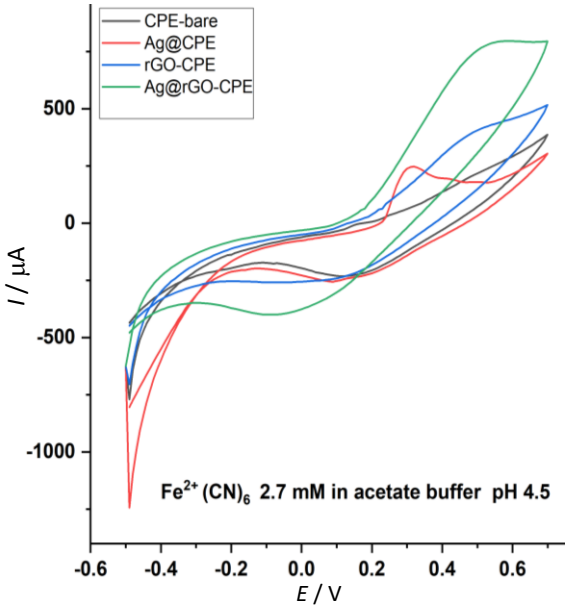

Figure 2. *Cyclic voltammograms of bare CPE, Ag@CPE, rGO-CPE and rGO@Ag-CPE recorded in 2.7 mM $[Fe(CN)_6]^{4-}$ in acetate buffer (pH 4.5) with 100 mV s^{-1} scan rate*

Across various configurations, the electrochemical response was most pronounced at the rGO@Ag-CPE electrode, exhibiting the highest redox peak currents and the lowest ΔE_p, defined as the peak-to-peak separation between the anodic and cathodic peaks.

The ΔE_p is a key indicator of electron-transfer kinetics, with lower values indicating faster, more reversible processes. The observed decrease in ΔE_p for rGO@Ag-CPE demonstrates that the combination of highly conductive rGO sheets and catalytic Ag nanoparticles produces a synergistic effect, enhancing both the charge-transfer efficiency and the effective electroactive surface area of the electrode. The application of $[Fe(CN)_6]^{3-}$ as a redox indicator has long been recognized for evaluating interfacial electron-transfer capabilities of modified electrodes due to its reversible outer-sphere electrochemical process and high sensitivity to surface conductivity [39,41,44]. The observed lowest ΔE_p values for rGO@Ag-CPE further support the successful modification of the carbon paste material, demonstrating enhanced electron-transfer kinetics and confirming the electrode's potential for highly sensitive and reliable electrochemical sensing.

Electrochemical behaviour of atenolol at rGO@Ag-CPE: a comparative voltammetric analysis

Based on physicochemical and electrochemical analyses, the rGO@Ag-CPE was selected as the optimal electrode for the electrochemical study of atenolol (ATN). The electrocatalytic performance of the doubly modified electrode was investigated and compared with CPE in a 100 mM H_2SO_4 solution, pH 2, using cyclic voltammetry (CV), square wave voltammetry (SWV), and differential pulse voltammetry (DPV).

As can be seen in Figure 3, the well-demarcated oxidation peak associated with the oxidation of atenolol ATN occurred at +1.45 V (*vs.* Ag/AgCl) in the three electrochemical methods, *i.e.* CV, SWV, and DPV. The intensity of the oxidation peak was higher on rGO@Ag-CPE than on the CPE, thereby indicating additional electrochemical reactivity on the former electrode. The combination of rGO and Ag nanoparticles is primarily responsible for the enhanced electrochemical reactivity of rGO@Ag-CPE, owing to the higher electroactive surface area, lower charge-transfer resistance, and easier electron-transfer processes at the electrode/electrolyte interface [16-18]. On the contrary, the CPE exhibited a broader, less resolved oxidation peak with a positive shift in the oxidation potential, indicating sluggish electron-transfer kinetics and larger overpotentials. The sharpness and resolution of the oxidation peaks in the DPV and SWV curves further substantiated the enhanced sensitivity of the rGO@Ag-CPE electrode, as evidenced by more prominent oxidation peaks with higher currents and higher signal-to-background ratios. The above attributes demonstrate the efficient electrocatalytic oxidation capability of the nanocomposite-CPE sensor electrode for ATN detection.

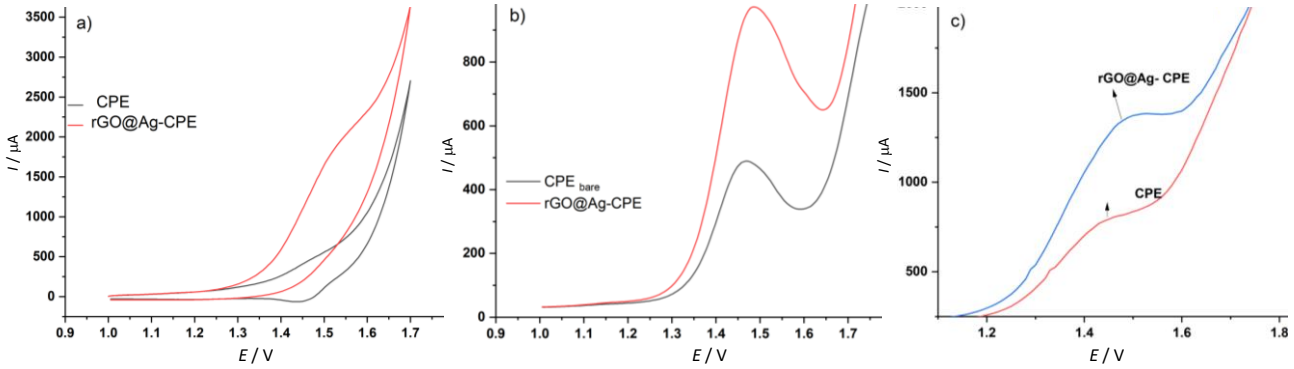

Figure 3. *(a) cyclic voltammograms, (b) square-wave voltammograms and (c) differential pulse voltammograms recorded in acidic medium (100 mM H_2SO_4, pH 2.0) in the presence of 1mM ATN, at bare CPE and rGO@Ag-CPE. Measurements were performed under optimized conditions: scan rate 100 mV s^{-1}, pulse amplitude 50 mV, frequency 25 Hz*

Proposed oxidation mechanism of atenolol

The electrochemical oxidation of atenolol (ATN) is widely reported to proceed through a 2-electron/2-proton mechanism, involving the transformation of the benzylic hydroxyl group (-CH(OH)-) into the corresponding ketone (-C=O). This assignment is strongly supported by the dependence of the anodic peak potential on pH, where reported slopes of approximately -53.6 mV pH^{-1} suggests that the number of transferred protons and electrons is equal, as predicted by the Nernst equation [22,24]. Within the rGO@Ag-CPE -modified electrode, AgNPs act as highly active electrocatalytic sites that promote fast charge transfer, while rGO contributes a large electroactive surface and enhances adsorption of ATN via π-π stacking and hydrogen-bonding interactions. The synergistic combination of rGO and AgNPs thus provides a highly efficient sensing platform. Figure 4 illustrates the proposed $2e^-/2H^+$ oxidation pathway of ATN at the modified electrode surface (adapted from references [34,37,50]).

Optimization of analytical parameters

The analytical performance of the rGO@Ag-CPE sensor for atenolol was strongly influenced by the experimental parameters. To obtain maximum sensitivity and a well-defined peak, it was necessary to optimize key parameters, including the supporting electrolyte, pH, scan rate (for CV studies), and frequency and pulse amplitude (for SWV studies).

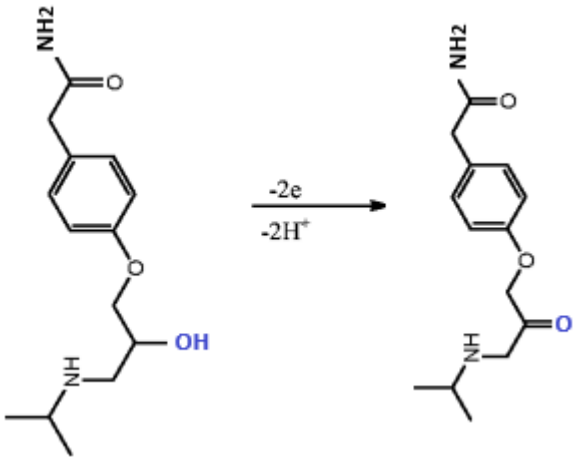

Figure 4. *Proposed oxidation mechanism of atenolol involving a $2e^-/2H^+$ process at the modified electrode surface. Adapted and redrawn based on references [22, 24]*

Effect of supporting electrolyte and pH on oxidation peak current

The influence of supporting electrolyte and pH on ATN oxidation was evaluated in four media (c_{ATN} = 323 µM): 0.1 M H_2SO_4 (pH 2), 0.1 M acetate buffer (pH 5), 0.1 M PBS (pH 7) and 0.1 M PB (pH 8). The oxidation peak current decreased with increasing pH (Figure 5). The highest current response was obtained in strongly acidic media (H_2SO_4, pH 2), while significantly lower responses were observed in neutral and basic media. Additionally, a noticeable shift in the oxidation peak potential was observed in acetate buffer (pH 5) and PBS (pH 7), which can be attributed to differences in buffer pH and ionic strength, which affect proton availability and the electrochemical environment. This behaviour is consistent with the proposed $2e^-/2H^+$ oxidation mechanism and with literature reports on the oxidation of β-blockers in various buffers. This behaviour can be explained by two main factors:

(i) Protonation state of ATN. ATN is fully protonated in strongly acidic media (base dissociation constant, pK_b ≈9.6), which enhances electrostatic attraction with the negatively charged rGO@Ag-CPE surface. This promotes adsorption and facilitates electron transfer, yielding higher oxidation currents.

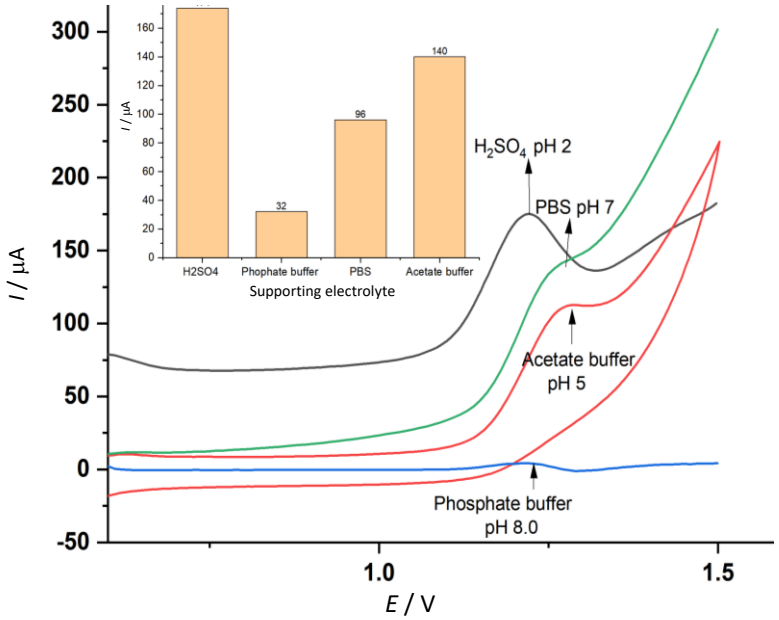

Figure 5. *SWVs and oxidation peak currents of atenolol (323 µM) at rGO@Ag-CPE in different supporting electrolytes: 0.1 M H_2SO_4 (pH 2), 0.1 M acetate buffer (pH 5), 0.1 M phosphate-buffered saline (pH 7) and 0.1 M phosphate buffer (pH 8)*

(ii) Higher solution conductivity in acidic conditions: H_2SO_4 provides the highest ionic conductivity among the tested electrolytes, minimizing solution resistance and accelerating charge transfer kinetics at the electrode surface. These observations are consistent with previous findings reporting enhanced electrochemical oxidation of β-blockers under acidic conditions due to improved protonation and favourable electrochemical kinetics [16,37,47,50]. Based on these results, 0.1 M H_2SO_4 (pH 2) was selected as the optimal supporting electrolyte for subsequent analysis.

Link between pH behaviour and oxidation mechanism

The strong dependence of oxidation current and potential on pH directly supports the proposed $2e^-/2H^+$ oxidation mechanism described in Figure 4. The observed decrease in current with increasing pH, along with the more favourable kinetics in proton-rich media, is consistent with a mechanism in which proton availability is essential for the transformation of the benzylic -CH(OH)- group into a carbonyl (-C=O). Therefore, the pH-dependent behaviour observed experimentally reinforces the mechanistic pathway proposed for ATN oxidation.

Based on these observations, 0.1 M H_2SO_4 (pH 2) was selected as the optimal supporting electrolyte for subsequent experiments, as it provides maximum sensitivity and favourable electrochemical kinetics.

Optimization of voltammetry parameters

After selecting a 100 mM H_2SO_4 solution at pH 2 as the supporting electrolyte, the voltammetric parameters for the oxidation of atenolol (323 µM) were optimized using CV and SWV. The pulse amplitude (10 to 100 mV), pulse frequency (3 to 30 Hz) and scan rate (50 to 150 mV s^{-1}) were systematically varied to maximize the oxidation current. The obtained results are summarized in Table 1.

Table 1. *The optimized voltammetry parameters for ATN detection at rGO@Ag-CPE in 100 mM H_2SO_4, pH 2*

Parameter	Tested range	Optimal value
Pulse amplitude, mV	10 to 100	50
Pulse frequency, Hz	3 to 30	25
Scan rate, mV s^{-1}	10 to 150	100

The peak currents *vs*. voltammetry parameter values are demonstrated in Figure 6, showing an optimal value of pulse amplitude of 50 mV, frequency of 25 Hz and scan rate of 100 mV s^{-1}. These optimal values were used in the final measurement to yield the highest sensitivity and reproducibility.

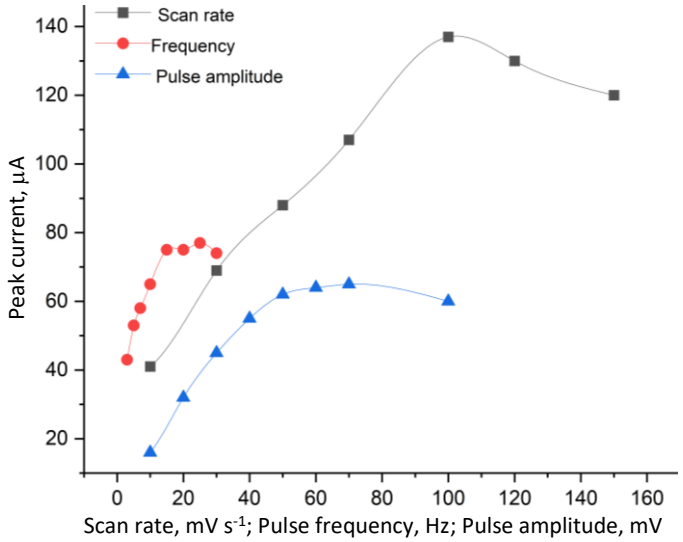

Figure 6*. Optimization of voltammetry parameters: pulse amplitude, frequency and scan rate for 323 µM ATN rGO@Ag-CPE in 100 mM H_2SO_4 (pH 2)*

Analytical performance and calibration of rGO@Ag-CPE sensor

The analytical performance of the modified rGO@Ag-CPE sensor for the quantitative determination of the target analyte (ATN) was evaluated under optimized experimental conditions in acidic medium (100 mM H_2SO_4, pH 2) using two electrochemical techniques, cyclic voltammetry (CV) and square wave voltammetry (SWV). Both CV and SWV techniques were employed to assess sensitivity, linearity, and detection capability across a wide concentration range, as illustrated by the recorded voltammograms and their corresponding calibration plots in Figures 7 and 8.

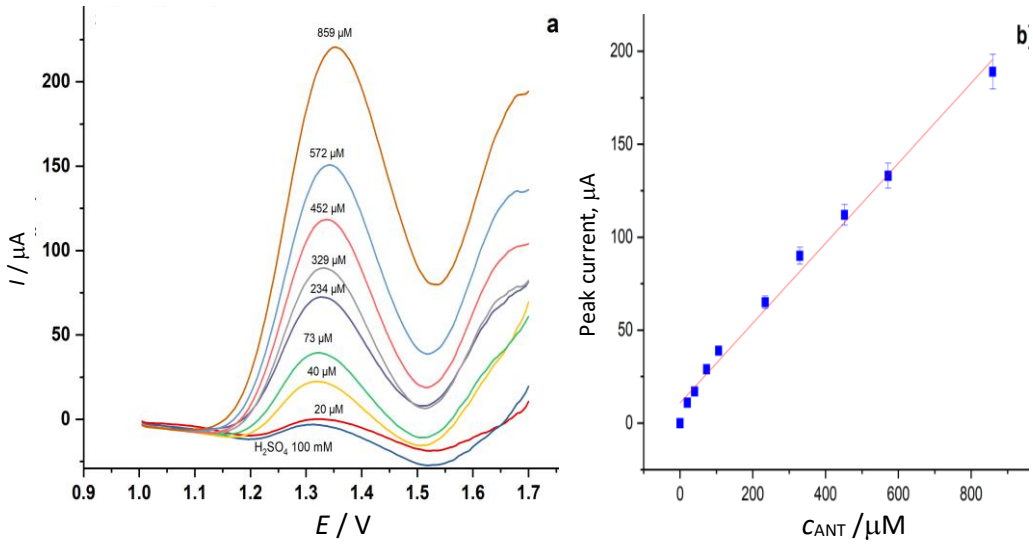

Figure 7. *a) Square-wave voltammetry (pulse amplitude 50 mV and frequency 25 Hz) responses of rGO@Ag-CPE sensor in 100 mM H_2SO_4 (pH 2) with increasing ATN concentrations from 20 to 859 µM, b) corresponding calibration plot constructed from triplicate measurements (mean ± SD)*

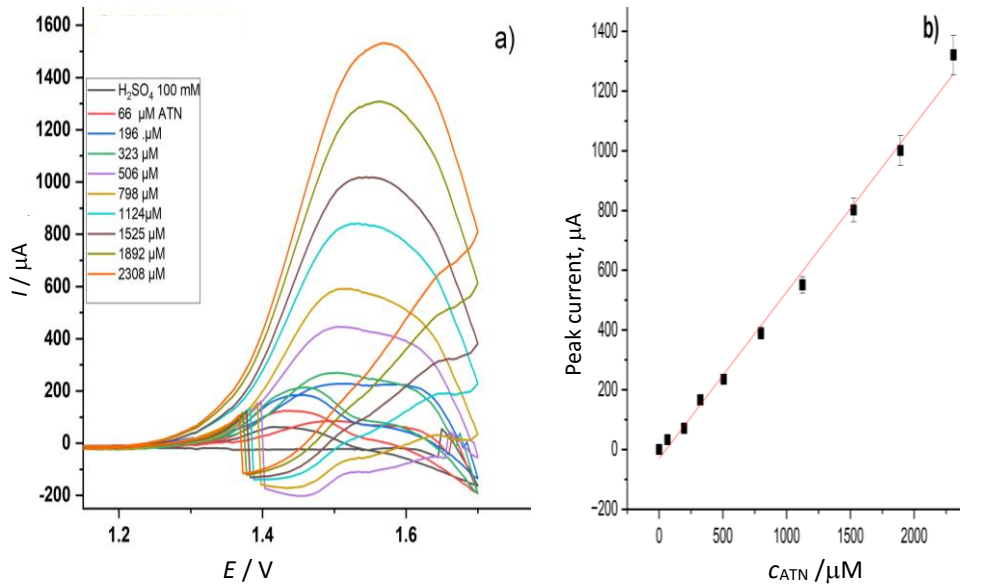

Figure 8. *a) Cyclic voltammetry responses of rGO@Ag-CPE in 100 mM H_2SO_4 (pH 2) with increasing ATN concentrations from 66 to 2308 µM, b) corresponding calibration plot constructed from triplicate measurements (mean ± SD)*

The SWV showed a clearly defined, symmetrical oxidation peak at approximately 1.35 V that was stable across the concentration range (20 to 859 µM). The oxidation peak current was linear with ATN concentration (y = 10.72 + 0215x; R^2 = 0.9953) and attained a low limit of detection (LOD) of 2.9 µM.

On the other hand, cyclic voltammetry showed higher absolute current peak values and good linearity (y = 0.56x - 30.6, R^2 = 0.9946) over a wide concentration range (66 to 2308 µM), with a

calculated sensitivity of 0.56 µA μM^{-1}. Nevertheless, the corresponding limit of detection (15 µM) was relatively high, possibly due to the capacitive current associated with the measurement. These results suggest that SWV is more suitable for trace analysis, whereas CV is applicable to mid- to high-concentration ranges. These observations can be further explained by a slight shift of the oxidation peak potential toward less positive values in SWV, which is advantageous for analytical performance. This shift reduces overpotential, minimizes interference, and provides a more defined and sensitive peak for ATN quantification, complementing the high current and wider concentration range measured by CV. The combined features of these techniques, along with the electrocatalytic property offered by the rGO@Ag nanocomposite, together prove the enhanced analytical performance and usefulness of the proposed sensor for accurate measurement of atenolol concentration in pharmaceutical and environmental samples.

The analytical performance of the proposed rGO@Ag-CPE electrochemical sensor was further compared with various previously published electrochemical sensors, electrochemical sensors with spectrofluorimetric validation, and chromatography-based methods for the analytical determination of ATN concentration in pharmaceutical preparations and natural waters (Table 2). The rGO@Ag-CPE electrochemical sensor provides a broad linear range of 20-859 µM with a relatively low LOD of 2.9 µM. While other methods can yield low LOD values in laboratory settings with considerable preparation before analysis and longer analysis times, the proposed electrochemical sensor offers an acceptable trade-off among LOD, linearity, and ease of preparation, with minimal equipment requirements.

***Table 2**. Comparison of analytical performance of various sensors and methods for atenolol determination*

Method / Sensor	Technique	Linear range, µM	LOD, µM	Material/electrode	Ref.
Spectrofluorimetry	Spectrofluorimetric method	0.38 to 7.51	0.12	Molecularly imprinted SPE sorbent	[53]
HPLC-Fluorescence detection	High-performance LC	1.88 to 75.1	0.01	—	[54]
Mordenite-modified CPE	DPV	0.4 to 80	0.10	Carbon paste electrode modified with mordenite	[55]
NPs/MWCNTs/GC	DPV	0.112 to 1.792	0.09	Gold nanoparticles + multiwalled carbon nanotubes on GCE	[56]
SPION-15%AC/GCE	DPV	1.21 to 285	0.40	Superparamagnetic iron oxide + activated carbon	[22]
MgO/SPE	DPV	6.66 to 909.09	1.76	Magnesium oxide	[57]
ZnO-doped GO / GCE	DPV	7.8 to 84 (plus 167 to 639)	2.50	ZnO nanoparticle-doped graphene oxide composite on glassy carbon electrode	[58]
rGO@Ag-CPE	SWV	20 to 859	2.90	Reduced graphene oxide + silver nanocomposite	This work

Repeatability and reproducibility of rGO@Ag-CPE

The repeatability and reproducibility of the rGO@Ag-CPE sensor were evaluated using SWV at a constant atenolol concentration of 323 µM. Repeatability was evaluated by conducting five consecutive analyses using a single identical rGO@Ag-CPE electrode on the same day under the same laboratory conditions; the data are presented in Figure 9A.

Reproducibility was evaluated by independently preparing four rGO@Ag-CPE electrodes using identical modification steps and testing them under identical conditions; the data are presented in Figure 9B. The calculated relative standard deviations for repeatability and reproducibility were 2.2% and 2.5%, respectively, which were well within the ICH-recommended limit of 5% for analytical validation of methods [46].

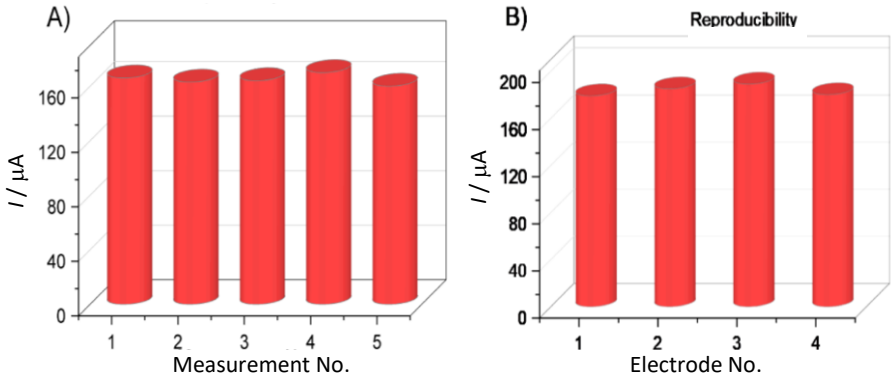

Figure 9. *A) Repeatability and B) reproducibility measurements for 323 µM ATN at rGO@Ag-CPE in 0.1 M H_2SO_4 (pH 2) using SWV under optimized conditions*

Analytical applications in real samples

The practical applicability of the rGO@Ag-CPE electrochemical sensor for atenolol determination was assessed in two types of real samples: pharmaceutical tablets and river water. The standard addition method was employed to minimize matrix effects and validate the accuracy of the procedure. Blank river water analyses confirmed the absence of ATN prior to spiking, while pharmaceutical tablets containing a defined ATN amount were analysed directly. Table 3 summarizes the results of ATN determinations in pharmaceutical tablets and river water samples.

Table 3. *Determination of ATN in real samples*

Sample		Amount, µM		Recovery, %	RSD[b], %	*t*-value (4.30[c])
		Added	Found[a]			
Tablet		0.0[d]	143			
		99	98.2 ± 0.5	99.2	0.4	3.46
		195	189.2 ± 3.4	97.0	1.7	3.14
River water	S1	0.0	n.d.[e]			
		340	335.1 ± 8.4	98.6	2.5	1.01
		503	502.1 ± 11.3	99.8	2.3	0.14
	S2	0.0	n.d.			
		340	301.2 ± 12.1	88.8	4.0	5.56
		503	498.7 ± 15.3	99.1	3.07	0.49
	S3	0.0	n.d.			
		340	339.1 ± 6.2	99.7	1.83	0.25
		503	504.3 ± 10.5	100.2	2.1	0.21
	S4	0.0	n.d.			
		340	346.8 ± 9.6	102.0	2.8	1.23
		503	510.5 ± 17.3	101.5	3.4	0.75

[a]Obtained from three repeated measurements; [b]Relative standard deviation; [c]Standard *t*-value for two degrees of freedom and 95 % confidence limit; [d]Real concentration of ATN was 125 µM; [e]Not detected

Recovery rates for the pharmaceutical formulations ranged from 97.0 to 99.2%, with RSD values as low as 0.4 %, demonstrating the accuracy of the proposed method in complex drug matrices. In river water samples, recoveries ranged from 88.8 to 102.0 % with RSD values of 1.8-4.0 %, confirming satisfactory reproducibility. Added versus found concentrations were compared using a student's t-test. Calculated t-values were lower than the critical value in most cases (4.30 at 95 % confidence, degree of freedom = 2), indicating that no significant systematic errors existed. Only for sample S2 at 340 µM did the t-value exceed the threshold, which is justified by matrix interferences inherent in environmental samples.

Overall, these findings indicate that the rGO@Ag-CPE sensor has reliable precision, accuracy, and selectivity. These factors make it appropriate for the determination of atenolol in pharmaceutical formulations and environmental water samples.

Conclusion

In this work, a rGO@Ag-CPE has been successfully prepared and employed for the voltammetric determination of atenolol. The decoration of Ag nanoparticles on rGO sheets enhanced its electron transfer rate and increased the electroactive surface area, which resulted in higher anodic responses compared to the bare CPE. A wide linear range, low detection limit, and good reproducibility were obtained. Recovery studies from pharmaceutical tablets (97.0 to 99.2 %) and spiked river water samples (88.8 to 102 %) were within the limits of accuracy and precision, and the calculated t-values were less than the critical limit. Compared with electrodes reported in the literature, rGO@Ag-CPE exhibits superior analytical performance while maintaining simplicity and low cost in its preparation. Thus, the proposed sensor in this study provides a convenient and scalable platform for sensing atenolol in pharmaceutical quality control and environmental applications, and the method could be extended to other β-blockers and pharmaceutical pollutants.

Conflict of Interest: *The authors declare no conflict of interest regarding the publication of this study.*

Acknowledgements: *The authors gratefully acknowledge support from the SUSNANO project (Twinning to boost the scientific and innovation capacity of the University of Tirana to develop sustainable nanosensors for water pollution detection, Grant No. 101059266-HORIZON-WIDERA-2021-ACCESS-02-01) for funding this research.*

References

[1] B. Rehman, D.P. Sanchez, P. Patel, S. Shah, *Atenolol*, StatPearls, Treasure Island, FL, 2024. https://www.ncbi.nlm.nih.gov/books/NBK539844

[2] M. Yi, Q. Sheng, Q. Sui, H. Lu, β-blockers in the environment: Distribution, transformation, and ecotoxicity, *Environmental Pollution* **266** (2020) 115269. https://doi.org/10.1016/j.envpol.2020.115269

[3] C. Steinbach, V. Burkina, G. Fedorova, K. Grabicova, A. Stara, J. Velisek, V. Zlabek, H. Schmidt-Posthaus, R. Grabic, H. Kocour Kroupova, The sub-lethal effects and tissue concentration of the human pharmaceutical atenolol in rainbow trout (*Oncorhynchus mykiss*), *Science of the Total Environment* **493** (2014) 1042-1051. https://doi.org/10.1016/j.scitotenv.2014.07.111

[4] Q. Xu, L. Luo, Z. Zhu, X. Liu, T.V. Ong, J.W.C. Wong, M. Pan, The fate of atenolol in wastewater treatment plants of representative densely urban agglomerations in China, *Journal of Environmental Quality* **54(1)** (2024) 204-216. https://doi.org/10.1002/jeq2.20653

[5] *Environmental Risk Assessment Data Atenolol*, AstraZeneca Sustainability Reports, 2023. https://www.astrazeneca.com/content/dam/az/PDF/Sustainability/era/Atenolol.pdf

[6] K. Fent, A. A. Weston, D. Caminada, Ecotoxicology of human pharmaceuticals, *Aquatic Toxicology* **76(2)** (2006) 122-159. https://doi.org/10.1016/j.aquatox.2005.09.009

[7] N. M. Vieno, H. Härkki, T. Tuhkanen, L. Kronberg, Occurrence of pharmaceuticals in river water and their elimination in a pilot-scale drinking water treatment plant, *Environmental Science & Technology* **41(14)** (2007) 5077-5084. https://doi.org/10.1021/es062720x

[8] M. R. Brunetto, Y. Delgado, S. Clavijo, Y. Contreras, D. Torres, C. Ayala, Development of a MSFIA sample treatment system as front end of GC-MS for atenolol and propranolol determination in human plasma, *Talanta* **132** (2015) 15-22. https://doi.org/10.1016/j.talanta.2014.08.056

[9] B. Yilmaz, S. Arslan, Determination of atenolol in human urine by using HPLC, *Separation Science and Technology* **53(1)** (2018) 50-57. https://doi.org/10.1002/sscp.201700023

[10] B. Yilmaz, S. Arslan, A. Asci, HPLC method for determination of atenolol in human plasma and application to a pharmacokinetic study in Turkey, *Journal of Chromatographic Science* **50(10)** (2012) 914-919. https://doi.org/10.1093/chromsci/bms090

[11] C. Laghlimi, A. Moutcine, A. Chtaini, J. Isaad, A. Soufi, Y. Ziat, H. Amhamdi, H. Belkhanchi, Recent advances in electrochemical sensors and biosensors for monitoring drugs and metabolites in pharmaceutical and biological samples, *ADMET & DMPK* **11(2)** (2023) 151-173. https://doi.org/10.5599/admet.1709

[12] M. Frigoli, M. P. Krupa, G. Hooyberghs, J. W. Lowdon, T.J. Cleij, H. Diliën, K. Eersels, B. van Grinsven, Electrochemical sensors for antibiotic detection: A focused review with a brief overview of commercial technologies, *Sensors* **24(17)** (2024) 5576. https://doi.org/10.3390/s24175576

[13] J. Baranwal, B. Barse, G. Gatto, G. Broncová, A. Kumar, Electrochemical Sensors and Their Applications: A Review, *Chemosensors* **10(9)** (2022) 363. https://doi.org/10.3390/chemosensors10090363

[14] S. O. Fakayode, P. N. Brady, C. Grant, V. Fernand Narcisse, P. Rosado Flores, C. H. Lisse, D. K. Bwambok, Electrochemical Sensors, Biosensors, and Optical Sensors for the Detection of Opioids and Their Analogs: Pharmaceutical, Clinical, and Forensic Applications, *Chemosensors* **12(4)** (2024) 58. https://doi.org/10.3390/chemosensors12040058

[15] A. V. Bounegru, A. Dinu Iacob, C. Iticescu, P. L. Georgescu, Electrochemical Sensors and Biosensors for the Detection of Pharmaceutical Contaminants in Natural Waters. A Comprehensive Review, *Chemosensors* **13(2)** (2025) 65. https://doi.org/10.3390/chemosensors13020065

[16] N. Broli, M. Vasjari, L. Vallja, A. Shehu, S. Duka, S. Cenolli, A carbon paste modified with banana tissue for determination of atenolol in pharmaceutical tablets, *Journal of Hygiene Engineering and Design* **37** (2022) 149-154.

[17] N. Broli, M. Vasjari, S. Cenolli, L. Vallja, S. Duka, A. Shehu, Electrochemical determination of antibiotics at nano-modified carbon paste electrode, *Journal of Hygiene Engineering and Design* **42** (2023) 204-209.

[18] N. Broli, M. Vasjari, L. Vallja, S. Duka, A. Shehu, S. Cenolli, Electrochemical determination of atenolol and propranolol using a carbon paste sensor modified with natural ilmenite, *Open Chemistry* **19(1)** (2021) 875-883. https://doi.org/10.1515/chem-2021-0071

[19] E. Hoxha, N. Broli, M. Vasjari, S. Cenolli, An electrochemical sensing platform based on a carbon paste electrode modified with a graphene oxide/TiO_2 nanocomposite for atenolol determination, *Engineering Proceedings* **73(1)** (2024) 1. https://doi.org/10.3390/engproc2024073001

[20] M. A. El-Shal, S. M. Azab, H. A. M. Hendawy, A facile nano-iron oxide sensor for the electrochemical detection of the anti-diabetic drug linagliptin in the presence of glucose and metformin, *Bulletin of the National Research Centre* **43(1)** (2019) 95. https://doi.org/10.1186/s42269-019-0132-8

[21] G. Maduraiveeran, B. R. Adhikari, A. Chen, Nanomaterials-based electrochemical detection of chemical contaminants, *RSC Advances* **4(109)** (2014) 63296-63323. https://doi.org/10.1039/C4RA10399H

[22] A.S. Agnihotri, M. Nidhin, Advanced electrochemical detection and profiling of the antihypertensive drug atenolol via a SPION-activated carbon nanocomposite interface, *Nanoscale Advances* **7(14)** (2025) 4397-4411. https://doi.org/10.1039/D5NA00314H

[23] Y. Shao, J. Wang, H. Wu, J. Liu, I.A. Aksay, Y. Lin, Graphene-based electrochemical sensors and biosensors: a review, *Electroanalysis* **22(10)** (2010) 1027-1036. https://doi.org/10.1002/elan.200900571

[24] S. Zhu, B. Dong, S. Zhou, Degradation of atenolol with electrochemical oxidation at mixed metal oxide electrodes assisted by UV photolysis, CLEAN - *Soil, Air, Water* **46(4)** (2018) 1700077. https://doi.org/10.1002/clen.201700077

[25] Y. Xu, Z. Liu, X. Zhang, Y. Wang, J. Tian, Y. Huang, Y. Ma, X. Zhang, Y. Chen, A graphene hybrid material covalently functionalized with porphyrin: Synthesis and optical limiting property, *Advanced Materials* **21(12)** (2009) 1275-1279. https://doi.org/10.1002/adma.200801617
[26] E. Er, H. Çelikkan, N. Erk, A novel electrochemical nano-platform based on graphene/platinum nanoparticles/Nafion composites for the electrochemical sensing of metoprolol, *Sensors and Actuators B* **238** (2017) 779-787. https://doi.org/10.1016/j.snb.2016.07.108
[27] A. Dehnavi, A. Soleymanpour, Titanium Dioxide/Multi-Walled Carbon Nanotubes Composite Modified Pencil Graphite Sensor for Sensitive Voltammetric Determination of Propranolol in Real Samples, *Electroanalysis* **33** (2021) 355-364. https://doi.org/10.1002/elan.202060132
[28] E. Makhado, W. M. Seleka, Innovative self-assembled silver nanoparticles on reduced graphene oxide hydrogel nanocomposite for improved electrochemical hydrogen generation and sensing, *Scientific Reports* **15** (2025) 28595. https://doi.org/10.1038/s41598-025-13976-3
[29] C. Khelifi, R. Aitout, L. Makhloufi, S. Mahouche-Chergui, Eco-friendly synthesis of rGO/AgNPs hybrid nanomaterial for an efficient electrochemical sensor: Simultaneous detection of paracetamol and caffeine in pharmaceuticals, *Microchemical Journal* **197** (2025) 113545. https://doi.org/10.1016/j.microc.2025.113545
[30] I. Ivanišević, The Role of Silver Nanoparticles in Electrochemical Sensors for Aquatic Environmental Analysis, *Sensors* **23** (2023) 3692. https://doi.org/10.3390/s23073692
[31] K. Hwa, T. S. K. Sharma, A. Ganguly, Design strategy of rGO-HNT-AgNPs based hybrid nanocomposite with enhanced performance for electrochemical detection of 4-nitrophenol, *Inorganic Chemistry Frontiers* **7** (2020) 1981-1994. https://doi.org/10.1039/D0QI00006J
[32] A. M. Santos, A. Wong, O. Fatibello-Filho, Simultaneous determination of salbutamol and propranolol in biological fluid samples using an electrochemical sensor based on functionalized-graphene, ionic liquid and silver nanoparticles, *Journal of Electroanalytical Chemistry* **824** (2018) 1-8. https://doi.org/10.1016/j.jelechem.2018.07.018
[33] D. R. Dreyer, S. Park, C. W. Bielawski, R. S. Ruoff, The chemistry of graphene oxide, *Chemical Society Reviews* **39** (2010) 228-240. https://doi.org/10.1039/B917103G
[34] W. Li, R. Xiao, J. Xu, et al., Insights into degradation of pharmaceutical pollutant atenolol via electrochemical advanced oxidation processes with modified Ti_4O_7 electrode: efficiency, stability and mechanism, *Water Research* **228** (2023) 115920. https://doi.org/10.1016/j.envres.2023.115920
[35] M. K. Angier, R. J. Lewis, A. K. Chaturvedi, D. V. Canfield, Gas chromatographic/mass spectrometric differentiation of atenolol, metoprolol, propranolol, and an interfering metabolite product of metoprolol, *Journal of Chromatography B* **805** (2004) 289-295. https://doi.org/10.1093/jat/29.6.517
[36] J. Wang, Electrochemical biosensors: Towards point of care cancer diagnostics, *Biosensors & Bioelectronics* **21** (2006) 1887-1892. https://doi.org/10.1016/j.bios.2005.10.027
[37] R. N. Hegde, P. Vishwanatha, S. T. Nandibewoor, Electro-oxidation and determination of atenolol, *Research Journal of Chemical Sciences* **11** (2021) 75-83.
[38] M. Pumera, Graphene-based nanomaterials and their electrochemistry, *Chemical Society Reviews* **39** (2010) 4146-4157. https://doi.org/10.1039/C002690P
[39] Q. Zhang, S. Ma, X. Zhuo, C. Wang, H. Wang, Y. Xing, Q. Xue, K. Zhang, An ultrasensitive electrochemical sensing platform based on silver nanoparticle-anchored three-dimensional reduced graphene oxide for rifampicin detection, *Analyst* **147** (2022) 2156-2163. https://doi.org/10.1039/D2AN00452F
[40] W. S. Hummers, R. E. Offeman, Preparation of graphitic oxide, *Journal of the American Chemical Society* **80** (1958) 1339. https://doi.org/10.1021/ja01539a017

[41] A. Bello, M. Fabiane, D. Dodoo-Arhin, K.I. Ozoemena, N. Manyala, Silver nanoparticles decorated on a three-dimensional graphene scaffold for electrochemical applications, *Journal of Physics and Chemistry of Solids* **75** (2014) 109-114. https://doi.org/10.1016/j.jpcs.2013.09.006
[42] N. Ahmad, A. S. Al-Fatesh, R. Wahab, M. Alam, A. H. Fakeeha, Synthesis of silver nanoparticles decorated on reduced graphene oxide nanosheets and their electrochemical sensing towards hazardous 4-nitrophenol, *Journal of Materials Science: Materials in Electronics* **31** (2020) 34305-34315. https://doi.org/10.1007/s10854-020-03747-3
[43] S. Chanarsa, J. Jakmunee, K. Ounnunkad, A bifunctional nanosilver reduced graphene oxide nanocomposite for label free electrochemical immunosensing, *Frontiers in Chemistry* **9** (2021) 631571. https://doi.org/10.3389/fchem.2021.631571
[44] M. A. Alam, Graphene based electrochemical biosensors for the detection of cardiac biomarkers, *Biosensors & Bioelectronics X* **20** (2024) 100515. https://doi.org/10.1016/j.biosx.2024.100515
[45] F. Hosseini, M. Bahmaei, M. Davallo, Electrochemical determination of propranolol, acetaminophen and folic acid in urine, and human plasma using Cu_2O-CuO/rGO/CPE, *Russian Journal of Electrochemistry* **57** (2021) 357-374. https://dx.doi.org/10.1134/S1023193521040054
[46] M. Thompson, S. L. R. Ellison, R. Wood, Harmonized guidelines for single-laboratory validation of methods of analysis (IUPAC Technical Report), *Pure and Applied Chemistry* **74** (2002) 835-855. https://doi.org/10.1351/pac200274050835
[47] S. Pruneanu, F. Pogacean, C. Grosan, E. M. Pica, L. C. Bolundut, A. S. Biris, Electrochemical investigation of atenolol oxidation and detection by using a multicomponent nanostructural assembly of amino acids and gold nanoparticles, *Chemical Physics Letters* **504** (2011) 56-61. https://doi.org/10.1016/j.cplett.2011.01.051
[48] L. Kulla, A. Ameda, M. Vasjari, N. Broli, A rapid electrochemical platform for detecting thiamethoxam using a Ni-rGO carbon paste composite, *Journal of Natural Sciences* **36** (2024) 95-115.
[49] A. Ameda, L. Kulla, M. Vasjari, N. Broli, Square wave anodic stripping voltammetric determination of Hg(II) using carbon paste electrode modified with -rGO@Au, *Journal of Natural Sciences* **36** (2024) 47-63.
[50] C. Xu, X. Wang, J. Zhu, Graphene-Metal Particle Nanocomposites, Journal of Physical Chemistry C 112(50) (2008) 19841-19845. https://doi.org/10.1021/jp807989b
[51] C. Park, R.S. Ruoff, Chemical methods for the production of graphenes, Nature Nanotechnology 4(4) (2009) 217-224. https://doi.org/10.1038/nnano.2009.58
[52] K. Kovács, T. Tóth, L. Wojnárovits, Evaluation of advanced oxidation processes for β-blockers degradation: A review, *Water Science and Technology* **84** (2021) 631-645. https://doi.org/10.2166/wst.2021.631
[53] Y. Gorbani, H. Yılmaz, H. Basan, Spectrofluorimetric determination of atenolol from human urine using high-affinity molecularly imprinted solid-phase extraction sorbent, *Luminescence* **32** (2017) 1391-1397. https://doi.org/10.1002/bio.3335
[54] O. H. Weddle, E. N. Amick, W. D. Mason, Rapid determination of atenolol in human plasma and urine by high-pressure liquid chromatography with fluorescence detection, *Journal of Pharmaceutical Sciences* **67(7)** (1978) 1048-1051. https://doi.org/10.1002/jps.2600670748
[55] M. Arvand, M. Vaziri, M. Vejdani, Electrochemical study of atenolol at a carbon paste electrode modified with mordenite type zeolite, *Materials Science and Engineering: C* **30** (2010) 709-714. https://doi.org/10.1016/j.msec.2010.03.002

[56] S. Sharma, N. Jadon, R. Jain, Development of electrochemical sensor for simultaneous quantification of atenolol and losartan potassium*, Nanoscience and Technology: Open Access* **5(2)** (2018) 1-13. https://doi.org/10.15226/2374-8141/5/2/00156

[57] M. Khairy, A. A. Khorshed, F. A. Rashwan, G. A. Salah, H. M. Abdel-Wadood, C. E. Banks, Simultaneous voltammetric determination of antihypertensive drugs nifedipine and atenolol utilizing MgO nanoplatelet modified screen-printed electrodes in pharmaceuticals and human fluids, *Sensors and Actuators B: Chemical* **252** (2017) 1045-1054. https://doi.org/10.1016/j.snb.2017.06.105

[58] E. M. Ayan, S. U. Karabiberoğlu, Z. Dursun, A practical electrochemical sensor for atenolol detection based on a graphene oxide composite film doped with zinc oxide nanoparticles, C*hemistrySelect* **5(28)** (2020) 8846-8852. https://doi.org/10.1002/slct.202001019